MHD effects on micropolar nanofluid flow over a radiative stretching surface with thermal conductivity

Srinivas Maripala[1] and Kishan Naikoti[2]

[1]Department of Mathematics, Sreenidhi Institute of Science and Technology, Ghatkesar, Hyd-501301
[2]Department of Mathematics, Osmania University, Hyd-07
_____

ABSTRACT

In this paper, an analysis is presented the effects of variable thermal conductivity and radiation on the flow and heat transfer of an electrically conducting micropolar nanofluid over a continuously stretching surface with varying temperature in the presence of a magnetic field considered. The surface temperature is assumed to vary as a power-law temperature. The governing conservation equations of mass, momentum, angular momentum and energy are converted into a system of non-linear ordinary differential equations by means of similarity transformation. The resulting system of coupled non-linear ordinary differential equations is solved by implicit finite difference method with the Thomas algorithm. The results are analyzed for the effect of different physical parameters such as magnetic parameter, microrotation parameter, Prandtl number, radiation parameter; Eckert number, thermal conductivity parameter, Brownian motion parameter, Thermophoresis parameter, Lewis number, and surface temperature parameter on the velocity, angular velocity, temperature and concentration fields are presented through graphs. Physical quantities such as skin friction coefficient, local heat, local mass fluxes are also computed and are shown in table.

Key words: Nanofluid, heat transfer, finite difference method, thermal conductivity.
_____

INTRODUCTION

The enhancement of thermal conductivity in nanofluids has attracted the interest of many researchers. The Boungiorno[1] model, Kuznetseov and Nield[2] studied the influence of nanoparticles on a natural convection boundary layer flow passing a vertical plate. They considered the temperature and nanoparticle fraction both to be constant along the wall and concluded that the reduced Nusselt number is a decreasing function of the nanofluid numbers Nr, Nb and Nt. The mixed convection boundary layer flow passing a vertical flat plate embedded in a porous medium filled with a nanofluid was studied by Ahmad and Pop.[3] Furthermore, Eastman et al.[4] used pure copper nanoparticles of size less than 10nm and achieved an increase of 40 in thermal conductivity for only 0.3 volume fraction of the solid dispersed in ethyleneglycal. Hwang et al.[5] studied a detailed discussion about the effects of thermal conductivities under static and dynamic conditions, energy transfer by nanoparticles dispersion, particles migration due to viscosity gradient, non-uniform shear rate, Brownian diffusion and thermopharesis on the enhancement of the convective heat transfer coefficient, which are discussed to understand convective heat transfer characteristics of water based nanofluids flowing through a circular tube.

The study of boundary layer flow and heat transfer over a stretching surface particularly in the field of nanofluid has achieved a lot of success in the past years because of its high thermal conductivity and large number of applications in industry and technology. After the pioneering work by Sakiadis , a large amount of literature is available on

_____

boundary layer flow of Newtonian and non-Newtonian fluids over linear and nonlinear stretching surfaces. The problem of laminar fluid flow which results from the stretching of a flat surface in a nanofluid was investigated numerically by Khan and Pop. Hassani investigated the boundary layer flow problem of a nanofluid past a stretching sheet analytically. Both the effect of Brownian motion and thermophoresis were considered simultaneously in this case. A numerical investigation on boundary layer flow induced in a nanofluid due to a linearly stretching sheet in the presence of thermal radiation and induced magnetic field was conducted by Gbadeyan et al. (2011).   Srinivas Maripala and Kishan Naikoti[6], investigated the effects of heat source/sink on MHD convection slip flow of a thermosolutal nanofluid in a saturated porous media over a radiating stretching sheet.

Modeling and analysis of the dynamics of micropolar fluids has been the field of very active research for the last few decades as this class of fluids represents, mathematically , many industrially important fluids such as paints, body fluids, polymers, colloidal fluids, suspension fluids etc. These fluids are defined as fluids consisting of randomly oriented molecules whose fluid elements undergo translational as well as rotational motions. The theory of micropolar fluids was developed by Eringen [7] and excellent reviews about the applications of micropolar fluids have been written by Airman et al. [8,9]. Recently, Mostafa A.A.Mahmoud [16] studied the thermal radiation effects on MHD flow of a micropolar fluid over a stretching surface with variable thermal conductivity on the boundary layer flow and heat transfer of an electrically conducting micropolar nanofluid over a semi infinite continuously stretching sheet with power-law variable variation in the surface temperature in the presence of radiation.

2. Basic equations:

Consider a steady two-dimensional micropolar nanofluid flow of an incompressible, electrically conducting, subject to a transverse magnetic field over a semi-infinite stretching plate with variable temperature in the presence of radiation. The x-axis is directed along the continuous stretching plate and points in the direction of motion. The y-axis is perpendicular to x-axis and to the direction of the slot (the z-axis) whence the continuous stretching plate issues. It is assumed that the induced magnetic field and the Joule heating are neglected. The fluid properties are assumed to be constant, except for the fluid thermal conductivity which is taken as a linear function of temperature. Then under the usual boundary layer approximations, the governing equations for the problem can be written as follows [10]:

$$\frac{\partial u}{\partial x} + \frac{\partial v}{\partial y} = 0 \tag{1}$$

$$u\frac{\partial u}{\partial x} + v\frac{\partial u}{\partial y} = v\frac{\partial^2 u}{\partial y^2} + K_1\frac{\partial \sigma}{\partial y} - \frac{\sigma B_0^2}{\rho}u \tag{2}$$

$$G_1\frac{\partial^2 \sigma}{\partial y^2} - 2\sigma - \frac{\partial u}{\partial y} = 0 \tag{3}$$

$$\rho c_p\left(u\frac{\partial T}{\partial x} + v\frac{\partial T}{\partial y}\right) = \frac{\partial}{\partial y}\left(k\frac{\partial T}{\partial y}\right) + \mu(\frac{\partial u}{\partial y})^2 - \frac{\partial q_r}{\partial y} + \tau[D_B\frac{\partial C}{\partial y}\frac{\partial T}{\partial y} + \frac{D_T}{T_\infty}\left(\frac{\partial T}{\partial y}\right)^2] \tag{4}$$

$$\frac{\partial C}{\partial t} + u\frac{\partial C}{\partial x} + v\frac{\partial C}{\partial y} = D_B\frac{\partial^2 C}{\partial y^2} + \frac{D_T}{T_\infty}\frac{\partial^2 T}{\partial y^2} \tag{5}$$

where $v = (\mu + S)/\rho$ is the apparent kinematic viscosity, μ is the coefficient of dynamic viscosity, S is a constant characteristic of the fluid, σ is the microrotation component, $K_1 = S/\rho(> 0)$ is the coupling constant, $G_1(> 0)$ is the microrotation constant, ρ is the fluid density, $u\ and\ v$ are the components of velocity along $x\ and\ y$ direction, respectively. T is the temperature of the fluid in the boundary layer, T_∞ is the temperature of the fluid far away from the plate, T_w is the temperature of the plate, k is the thermal conductivity, c_p is the specific heat at constant pressure, σ_0 is the electric conductivity, B_0 is an external magnetic field and q_r is the radiative heat flux. T is the temperature, C is the concentration of the fluid, C_p is the specific heat, q_r is the radiative heat flux, T_w and C_w - the temperature and concentration of the sheet, T_∞ and C_∞- the ambient temperature and concentration, D_B - the Brownian diffusion coefficient, D_T the thermophoresis coefficient, B_0 - the magnetic induction, $(\rho C)_p$ - the heat capacitance of the nanoparticles, $(\rho C)_f$- the heat capacitance of the base fluid, and $\tau = (\rho C)_p/(\rho C)_f$ is the ratio between the effective heat capacity of the nanoparticles material and heat capacity of the fluid.

The boundary conditions of the problem are given by
$$y = 0\ u = \propto x\ v = 0\ T = T_w(x)\ \sigma = 0$$
$$y \to \infty,\ u \to 0,\ T \to T_\infty, \sigma \to 0 \tag{6}$$

_____

The wall temperature is assumed to vary along the plate according to the following power-law

$$T_w - T_\infty = \beta x^\gamma \tag{7}$$

where β and γ (the surface temperature parameter) are constants. The fluid thermal conductivity is assumed to vary as a linear function of the temperature in the form [11]

$$k = k_\infty [1 + b[(T - T_\infty)]] \tag{8}$$

where b is a constant depending on the nature of the fluid and k_∞ is the ambient thermal conductivity. In general, b>0 for air and liquids such as water, while b<0 for fluids such as lubrication oils. Using Rosselant approximation [12] we have

$$q_r = (-4\sigma^*/3k^*)\frac{\partial T^4}{\partial y} \tag{9}$$

where σ^* is the Stefan Boltzmann constant and k^* is the mean absorption coefficient. In this study, we consider the case where the temperature differences within the flow are sufficiently small. Expanding T^4 in a Taylor series about T_∞ and neglecting higher order terms [10], we have

$$T^4 \cong 4T_\infty^3 T - 3T_\infty^4 \tag{10}$$

Using Eq.(8), Eq.(4) becomes

$$\rho c_p \left(u\frac{\partial T}{\partial x} + v\frac{\partial T}{\partial y} \right) = \frac{\partial}{\partial y}\left(k\frac{\partial T}{\partial y} \right) + \mu\left(\frac{\partial u}{\partial y}\right)^2 + \frac{16\sigma^* T_\infty^3}{3k^*}\frac{\partial^2 T}{\partial y^2} + \tau[D_B \frac{\partial C}{\partial y}\frac{\partial T}{\partial y} + \frac{D_T}{T_\infty}\left(\frac{\partial T}{\partial y}\right)^2] \tag{11}$$

by using the following similarity transformations

$$\eta = (\alpha/v)^{\frac{1}{2}} y \, , \quad \psi = (\alpha v)^{\frac{1}{2}} x f(\eta),$$
$$u = \frac{\partial \psi}{\partial y}, \quad v = -\frac{\partial \psi}{\partial x}, \quad \sigma = (\alpha^3/v)^{1/2}xg(\eta), \quad \theta(\eta) = \frac{T-T_\infty}{T_w-T_\infty}, \quad k = k_\infty(1 + S\theta) \tag{12}$$

Substituting from Eq.(12) into Eqs.(1)-(3) and (10), we have

$$f''' + ff'' - f'^2 + G_1 g' - Mf' = 0 \tag{13}$$

$$G g'' - (2g + f'') = 0 \tag{14}$$

$$[4 + 3F(1 + S\theta)]\theta'' + 3FPr[f\theta' - \gamma f'\theta + Ec(f'')^2 + 3FS(\theta'')^2 + Pr[Nb \, \theta'\varphi' + Nt \, \theta'^2] = 0 \tag{15}$$

$$\varphi'' - Le f\varphi' + \frac{Nt}{Nb}\theta'' = 0 \tag{16}$$

Where
$G_1 = K_1/v$ (coupling constant parameter)
$M = (\sigma_0 B_0^2)/\rho a$ (magnetic parameter)
$G = G_1 \propto/v$ (microrotation parameter)
$P_r = (\mu c_p)/k_\infty$ (Prandtl number)
$F = (k_\infty k^*)/(4\sigma^* T_\infty^3)$ (Radiation parameter)
$Ec = \frac{\propto^2 x^2}{c_p(T_w - T_\infty)}$ (Eckert number)
$S = b(T_w - T_\infty)$ (thermal conductivity parameter)
$Nb = \tau D_B(C_w - C_\infty)/v$ (Brownian motion parameter)
$Nt = \tau D_T(T_w - T_\infty)/vT_\infty$ (Thermophoresis parameter)
$Le = v/D_B$ (Lewies number)
γ = Surface temperature parameter

For air 0≤S≤6, for water 0≤S≤0.12 and for lubrication oils -0.1≤S≤0 [13]

_____

The transformed boundary conditions are given by

$$f(0) = 0, f'(0) = 1, \ \theta(0) = 1 \ , g(0) = 0 \ ,$$
$$f'(\infty) = 0, (\infty) = 0 \ , g(\infty) = 0 \qquad\qquad (17)$$

In the above equations a prime denotes differentiations with respect to η. In the case of Newtonian fluid,

From the velocity field we can study the wall shear stress, τ_w as given by [14]:
$$\tau_w = -| \ (\mu + S)\frac{du}{dy} + S\sigma \ | \ at \ y = 0 \qquad\qquad (18)$$

The skin frication coefficient c_f is given by

$$c_f = \left(\frac{2\tau}{\rho u^2}\right)_{y=0} = -2R_{ex}^{-1/2}f''(0) \qquad\qquad (19)$$

where $R_{ex} = \alpha x/v$ is the local Reynolds number. Eq. (19) shows the skin frication coefficient does not contain the microrotation term in an explicitly way.

The rate of heat transfer is given by
$$q_{w=} - k\left(\frac{\partial T}{\partial y}\right) at \ y = 0 \qquad\qquad (20)$$

The local heat transfer coefficient is given by
$$h(x) = \ q_w \ /T_w - T_\infty \qquad\qquad (21)$$

The local Nusselet number is known as
$$N_{ux} = \frac{hx}{k} = -R_{ex}^{\frac{1}{2}}\theta'(0) \qquad\qquad (22)$$

The couple stress is given by
$$m_{w=} \ G_1 \ \left(\frac{\partial \sigma}{\partial y}\right)_{y=0} = \ R_{ex}\left(\frac{G_1\alpha}{x}\right)g'(0) \qquad\qquad (23)$$

Table 1: Values of $-f''(0), g'(0) , -\theta'(0) , -\varphi'(0)$ with G = 0.1, Pr 0.72, Ec=0.1, G =3,Le=0.1, Nb=Nt=0.1

M	F	γ	S	$-f''(0)$	$g'(0)$	$-\theta'(0)$	$-\varphi'(0)$
0.0	1.0	1.0	0.1	1.12845	0.261526	0.369843	0.35294
3.0	3.0	1.5	0.2	1.52926	0.294128	0.291427	029129
5.0	5.0	2.0	0.5	2.30121	0.351692	0.243161	0.24321

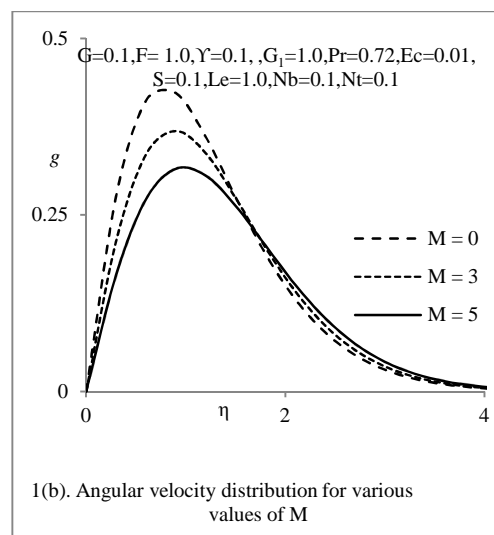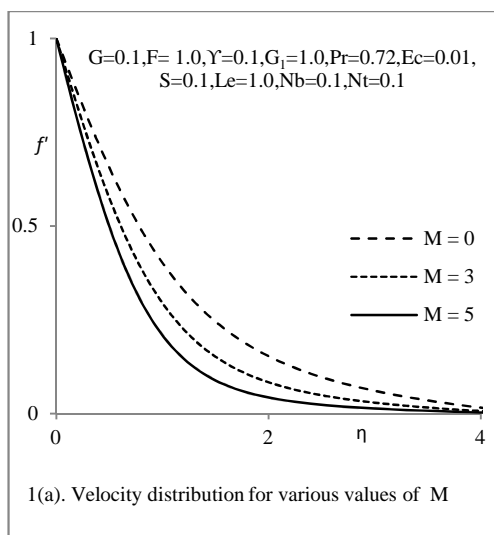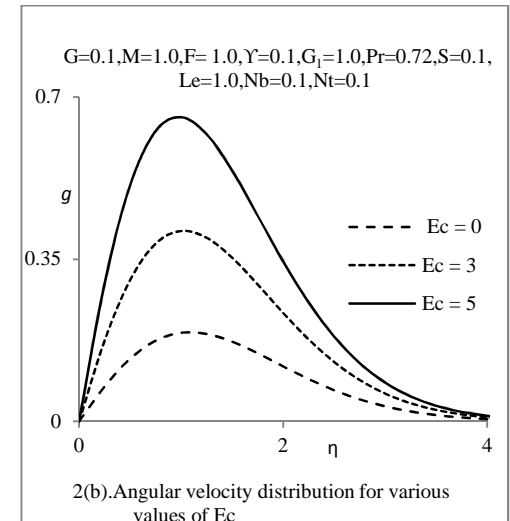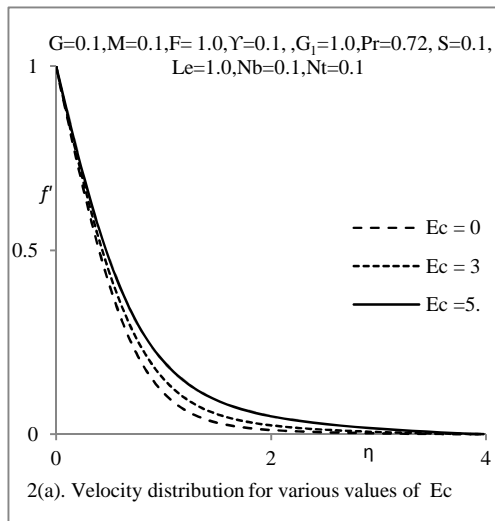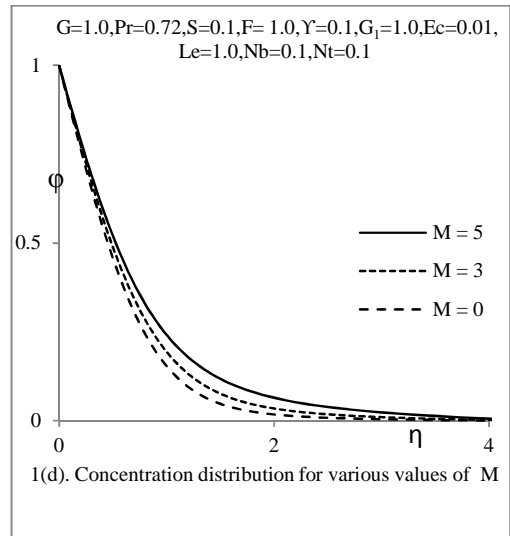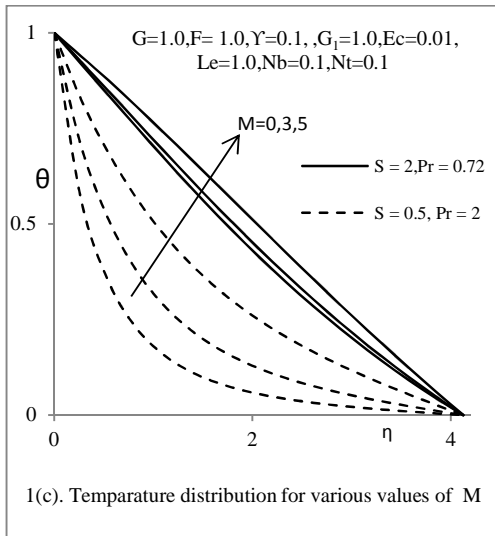**RESULTS AND DISCUSSION**

In order to solve the non-linear coupled equations (13) - (16) along with boundary conditions (17) an implicit finite difference scheme of Cranck-Nicklson type has been employed. The computations have been carried out for various flow parameters such as magnetic parameter *M*, microrotation parameter *G*, Prandtl number *Pr*, radiation parameter *F*, Eckert number *Ec*, thermal conductivity parameter *S*, Brownian motion parameter *Nb*, Thermophoresis parameter *Nt*, Lewies number *Le*, Surface temperature parameter γ on the velocity, angular velocity, temperature and concentration fields are presented through graphs. Physical quantities such as skinfrication coefficient $f''(0)$, the couple stress coefficient $-g'(0)$, local nusselet number $\theta'(0)$, and Sherwood parameter $\varphi'(0)$ are also computed and are shown in table. It is evident that with the increase of magnetic parameter *M*, radiation parameter *F*, surface temperature γ and thermal radiative parameter *S*, increases skin frication coefficient $f''(0)$, and couple stress coefficient $-g'(0)$, decreases the local nusselet number $\theta'(0)$ and Sherwood parameter $\varphi'(0)$.
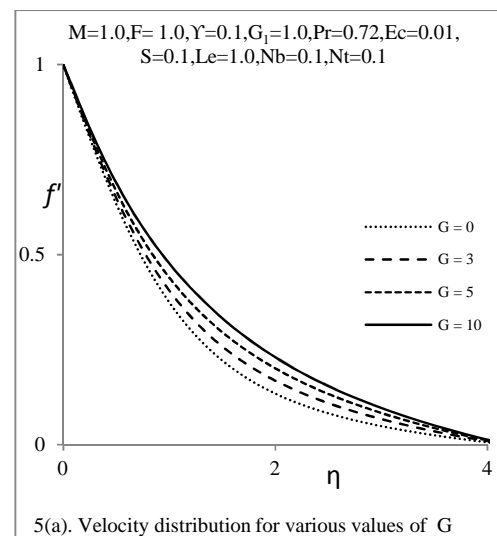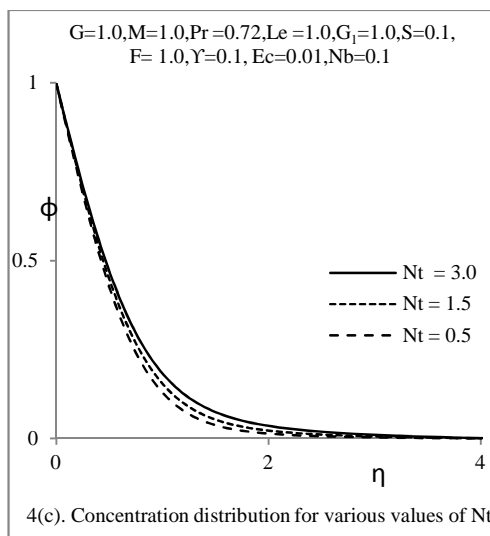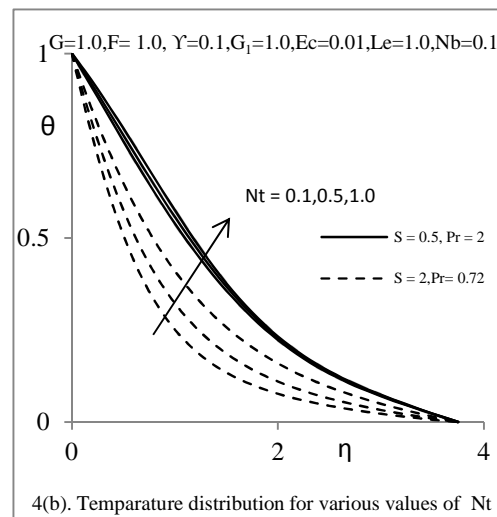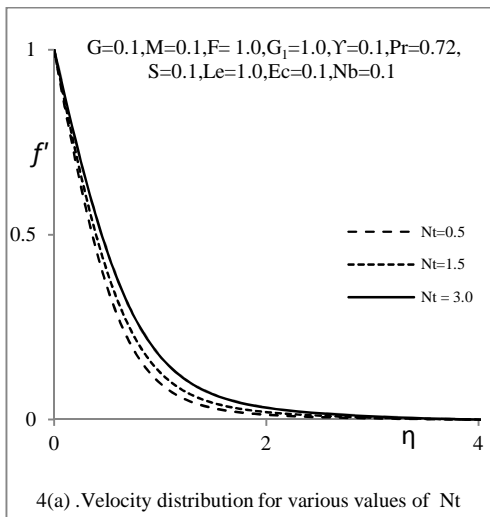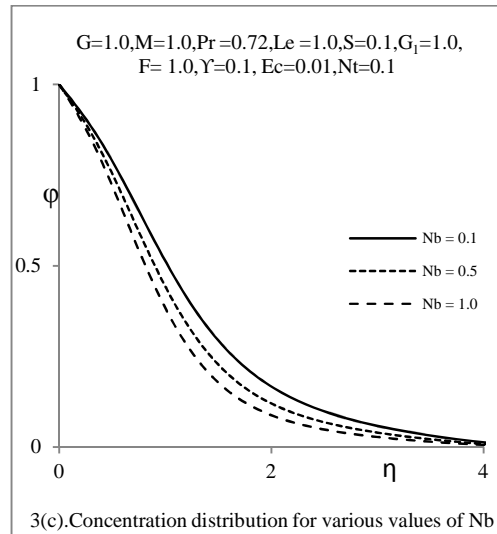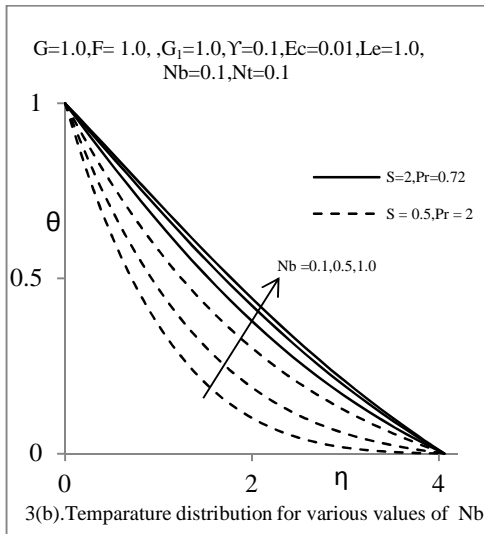
It is observed from Figure 1(a)-1(d),that an increase in magnetic parameter *M* leads to a decrease in velocity profiles *f′* and angular velocity *g*. The velocity boundary layer thickness becomes thinner as *M* increases. This is due to the fact that applications of a magnetic field to an electrically conductivity fluid produce a drag-like force called Lorentz force. This force causes reduction in the fluid velocity. The thermal boundary layer thickness increases with increasing the magnetic parameter *M* has shown in figure 1(c). The reason for this behavior is that the Lorentz force increases the temperature. The concentration profiles are increased with the increase of magnetic field parameter *M*, is observed from Figure 1(d). Figure 2 shows the Eckert number *Ec* effect on velocity, angular velocity and concentration profiles in the micropolar fluid flow. It can be see Figures 2(a), 2(b) and 2(c) that the velocity, angular velocity and temperature curves increase with the increase of Eckert number Ec. The effect of Brownian motion parameter *Nb* on velocity, temperature and concentration profiles are shown in figures 3(a) - 3(c). The velocity profiles are decreased with the increase of Brownian motion parameter *Nb*. Figure 3(b), illustrates that the temperature profiles are increased as Brownian motion parameter *Nb* increases. Concentration profiles are decreased, when Brownian motion parameter *Nb* increases is observed from the Figure 3(c).
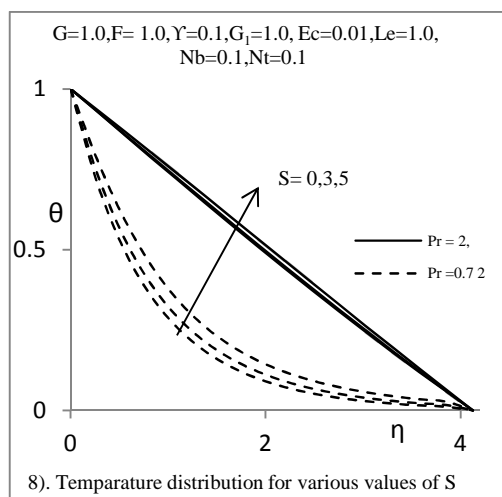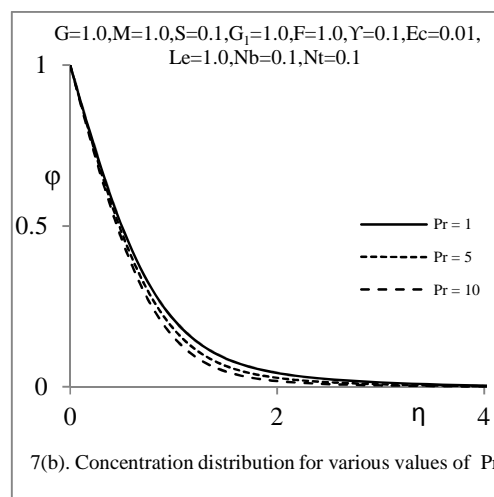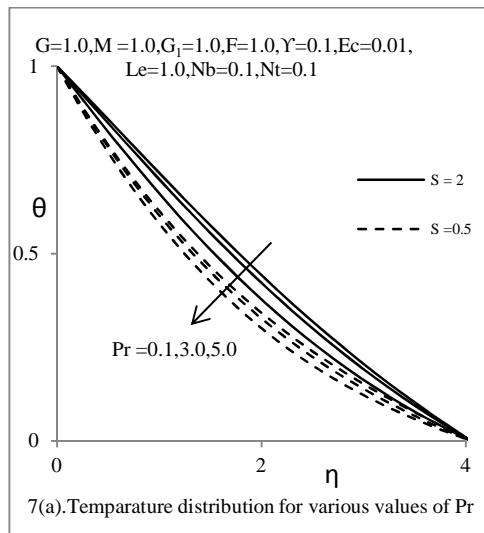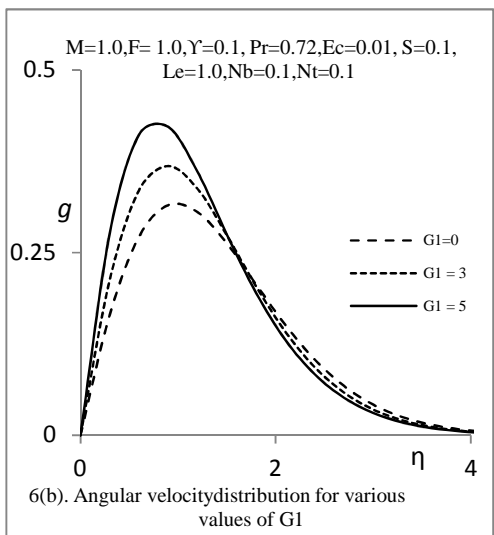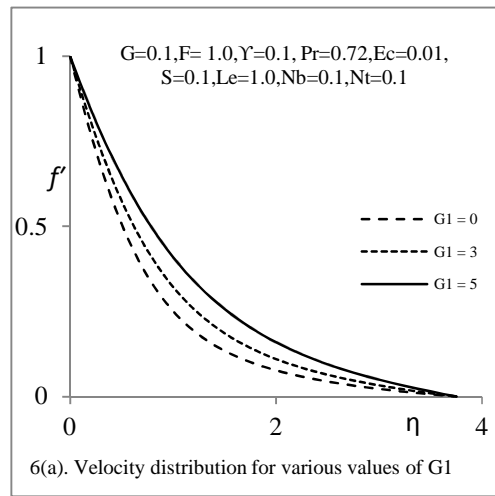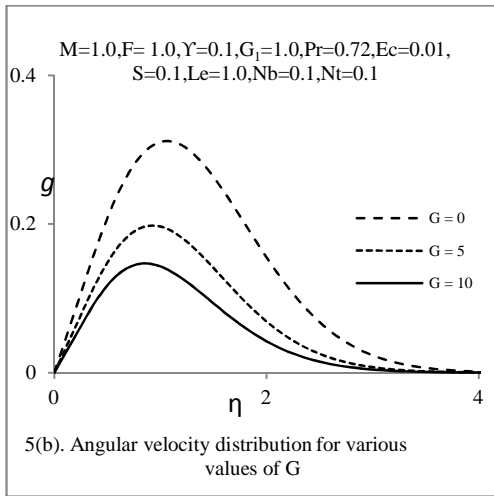
Figures 4(a) - 4(c) present typical profile for temperature and concentration for various values of thermophoretic parameter *Nt*. It is observed that an increase in the thermophoretic parameter leads to increase in fluid temperature and nanoparticle concentrations. The microrotation parameter *G* effects are explained in Figures 5(a) and 5(b). Velocity and angular velocity distribution profiles are increased when microroatation parameter *G* increases. Same phenomenon is observed in 6(a) and 6(b). That is the coupling constant *G1* effect is to increase velocity and angular velocity profiles. Figures 7(a) and 7(b) depict temperature profile θ and concentration profile φ, for different values of Prandtl number *Pr*. One can find that temperature of nanofluid particles decreases with the increase in *Pr* for both the cases *S=2* and *S=0.5*, which implies viscous boundary layer is thicker than the thermal boundary layer and the reverse phenomenon is observed from Figure 7(b). That is the concentration profiles are decreased as Prandtl number *Pr* increases. Fig. 8 shows the effect of the thermal conductivity parameter *S* on the temperature. From this figure it is noticed that the temperature decreases with the increasing of *S*. The variation of the temperature θ with respect to η for different values of *F* is plotted and shown in Fig.9. From Fig.9 one sees that the temperature decreases with θ increasing the radiation parameter *F*. The reason of this trend can be explained as follows. The effect of radiation is to decrease the rate of energy transport to the fluid, thereby decreasing the temperature of the fluid. Fig.10 illustrates the effect of the surface temperature parameter γ on the temperature distribution θ. From Fig.10, it is observed that the temperature decreases as γ increases. Lewies number *Le* effects are seen in Figure11, that is the Lewies number *Le*, decreases the concentration profiles when it increases.

5. Graphs:

1(a). Velocity distribution for various values of M

1(b). Angular velocity distribution for various values of M

_____

G=1.0,F= 1.0,ϒ=0.1, ,G$_1$=1.0,Ec=0.01,
Le=1.0,Nb=0.1,Nt=0.1

M=0,3,5

S = 2,Pr = 0.72
S = 0.5, Pr = 2

1(c). Temparature distribution for various values of M

G=1.0,Pr=0.72,S=0.1,F= 1.0,ϒ=0.1,G$_1$=1.0,Ec=0.01,
Le=1.0,Nb=0.1,Nt=0.1

M = 5
M = 3
M = 0

1(d). Concentration distribution for various values of M

G=0.1,M=0.1,F= 1.0,ϒ=0.1, ,G$_1$=1.0,Pr=0.72, S=0.1,
Le=1.0,Nb=0.1,Nt=0.1

Ec = 0
Ec = 3
Ec =5.

2(a). Velocity distribution for various values of Ec

G=0.1,M=1.0,F= 1.0,ϒ=0.1,G$_1$=1.0,Pr=0.72,S=0.1,
Le=1.0,Nb=0.1,Nt=0.1

Ec = 0
Ec = 3
Ec = 5

2(b).Angular velocity distribution for various
values of Ec

G=1.0,F= 1.0,ϒ=0.1,G$_1$=1.0,Le=1.0,Nb=0.1,Nt=0.1

S = 2,Pr = 0.72
S = 0.5,Pr = 2

Ec =0,3,5

2(c). Temparature distribution for various values of Ec

G=0.1,M=0.1,F= 1.0,ϒ=0.1,G$_1$=1.0,Pr=0.72,S=0.1,
Le=1.0,Ec=0.1,Nt=0.1

Nb = 0.5
Nb = 1.5
Nb = 3.0

3(a). Velocity distribution for various values of Nb

78

G=1.0,F= 1.0, ,G$_1$=1.0,Y=0.1,Ec=0.01,Le=1.0, Nb=0.1,Nt=0.1

3(b).Temparature distribution for various values of Nb

G=1.0,M=1.0,Pr =0.72,Le =1.0,S=0.1,G$_1$=1.0, F= 1.0,Y=0.1, Ec=0.01,Nt=0.1

3(c).Concentration distribution for various values of Nb

G=0.1,M=0.1,F= 1.0,G$_1$=1.0,Y=0.1,Pr=0.72, S=0.1,Le=1.0,Ec=0.1,Nb=0.1

4(a) .Velocity distribution for various values of Nt

G=1.0,F= 1.0, Y=0.1,G$_1$=1.0,Ec=0.01,Le=1.0,Nb=0.1

4(b). Temparature distribution for various values of Nt

G=1.0,M=1.0,Pr =0.72,Le =1.0,G$_1$=1.0,S=0.1, F= 1.0,Y=0.1, Ec=0.01,Nb=0.1

4(c). Concentration distribution for various values of Nt

M=1.0,F= 1.0,Y=0.1,G$_1$=1.0,Pr=0.72,Ec=0.01, S=0.1,Le=1.0,Nb=0.1,Nt=0.1

5(a). Velocity distribution for various values of G

_____

5(b). Angular velocity distribution for various values of G

6(a). Velocity distribution for various values of G1

6(b). Angular velocitydistribution for various values of G1

7(a).Temparature distribution for various values of Pr

7(b). Concentration distribution for various values of Pr

8). Temparature distribution for various values of S

_____

9). Temparature distribution for various values of F

10).Temparature distribution for various values of ϒ

11). Concentration distribution for various values of Le
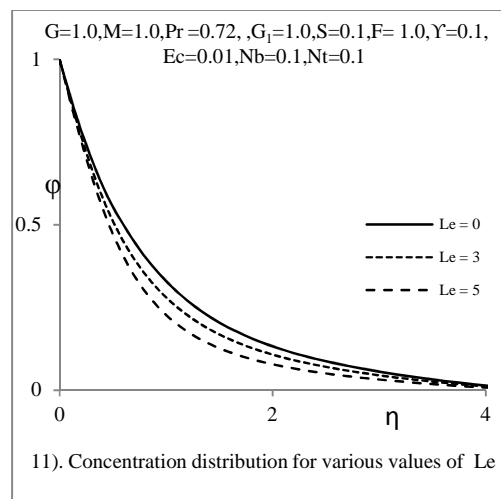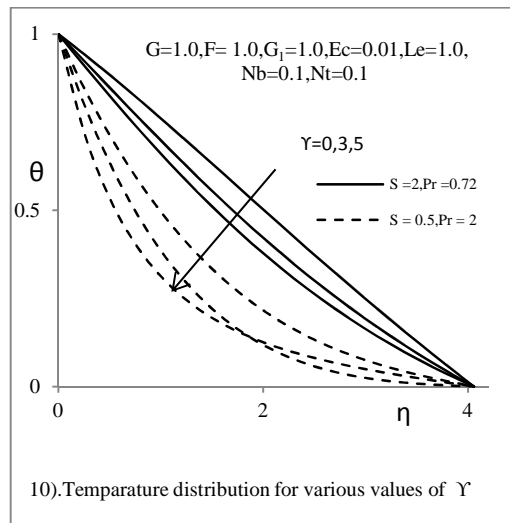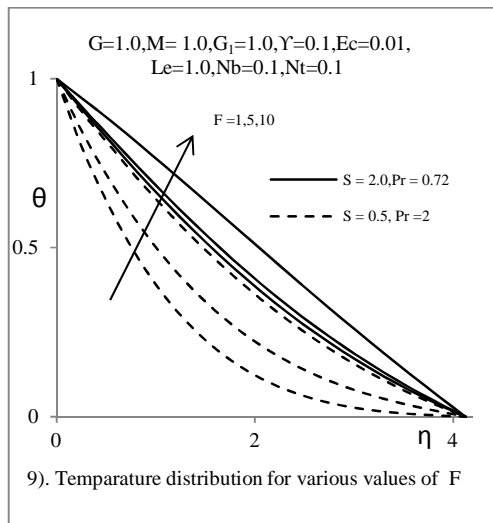
REFERENCES

[1] Buongiorno J, **2006** *ASME J. Heat Transfer* 128- 240

[2] Kuznetsov A V and Nield D A, **2010** *Int. J. Theor. Sci.* 49 243

[3] Ahmad S and Pop I, **2010** *Int. Commun. Heat Mass Transfer* 37 987

[4] Eastman J A, Choi S U S, Li S, Yu W and Thompson L J, **2001** *Appl. Phys. Lett*. 78 718

[5] Hwang K S, Jang S P and Choi S U S **2009** *Int. J. Heat Mass Transfer* 52 193

[6] Srinivas maripala and Kishan Naikoti, "MHD convection slip flow of a thermosolutal nanofluid in a saturated porous media over a radiating streaching sheet with heat source/sink", **2015**, Pushpa publications 18(2) pp177-198

[7] A.C. Eringen, *Math. Mech.* 6 (**1966**) 1–18.

[8]. T.Ariman, M.A.Turk and N.D.Sylvester, *Int. Jour. Engg. Sci.,* 11(**1973**), 905-930.

[9]. T.Ariman, M.A.Turk and N.D.Sylvester, *Int. Jour. Eng.Sci*., 12(**1974**), 273-293.

[10] A. Raptis, *Int. J. Heat Mass Transfer* 41(**1998**) 2865–2866.

[11] J.C. Slattery, Momentum, Energy and Mass Transfer in Continua, McGraw-Hill, New York, **1972**.

[12] E.M. Sparrow, R.D. Cess, Radiation Heat Transfer, Hemisphere Publishing Corporation, Washington, DC, **1978**.

[13] H. Schlichting, Boundary Layer Theory, Mc.Graw-Hill, New York, **1968**.

[14] V.M. Soundalgekar, H.S. Takhar,(**1983**), *Int. J. Eng. Sci*. 21, 961–965.

Srinivas Maripala and Kishan Naikoti   *Adv. Appl. Sci. Res., 2016, 7(3): 73-82*

82

_____

[15]. Srinivas Maripala and Kishan Naikoti, (**2016**), *International Journal of Mathematics Research*, Vol.5(1), pages 40-57.

[16] Mostafa A.A.Mahmoud, *physica* A 375(**2007**) 401-410.